$$\sigma_\theta^I = \frac{E}{t_T E^*} N_\theta^I + \frac{E}{1-\nu^2}\left[\nu\left(\varepsilon_r^* - \varepsilon_r^i\right) + \left(\varepsilon_\theta^* - \varepsilon_\theta^i\right)\right] \tag{21}$$

where N_r^I and N_θ^I are given by Eqs. (18) and (19). For the axisymmetric isotropic actuation with constant actuation strain in the actuator, i.e., ε_r^i and $\varepsilon_\theta^I = \varepsilon_a^i$, and zero actuation strain in the plate, the expressions for the stresses simplify. In the actuators, we get

$$\sigma_{ra}^I = -\frac{E}{r^2}\int_A^r \varepsilon^* \rho \, d\rho + \frac{E\left(\varepsilon^* - \varepsilon_a^i\right)}{1-\nu}$$

$$\sigma_{\theta a}^I = \frac{E}{r^2}\int_A^r \varepsilon^* \rho \, d\rho + \frac{E\left(\nu\varepsilon^* - \varepsilon_a^i\right)}{1-\nu} \tag{22}$$

while in the plate we get

$$\sigma_{rp}^I = -\frac{E}{r^2}\int_A^r \varepsilon^* \rho \, d\rho + \frac{E\varepsilon^*}{1-\nu}$$

$$\sigma_{\theta p}^I = \frac{E}{r^2}\int_A^r \varepsilon^* \rho \, d\rho + \frac{\nu E\varepsilon^*}{1-\nu} \tag{23}$$

These equations were compared with finite element calculations and close agreement was observed.

Note that Eqs. (22) and (23) predict nonzero radial stresses at the hole boundary, $r = A$. This incorrect prediction is due to the two-dimensional analysis. Thus, we can expect that the above equations provide reasonable results only at a small distance away from the hole. For the full thickness, we have only actuators and $\beta = 1$ and the induced stresses are obtained from Eqs. (22) as

$$\sigma_r^i = -\frac{E}{r^2}\int_A^r \varepsilon^i \rho \, d\rho, \quad \sigma_\theta^i = \frac{E}{r^2}\int_A^r \varepsilon^i \rho \, d\rho - E\varepsilon^i \tag{24}$$

The above stress expressions for the full-thickness actuation are the same as those obtained in Ref. 3.

Discussion

The mechanical stresses in the plate peak at the edge of the hole at $\theta = 90$ deg where $\sigma_\theta = 3S$ for a stress concentration factor of 3. The variation of stress concentration factor in the plate near the edge of the hole at $\theta = 90$ deg with normalized actuation strains for full-thickness and partial-thickness actuations are shown in Figs. 2 and 3 for maximum shear stress and Von-Mises stress criteria, respectively.

In the case of full-thickness actuation, when positive actuation strains are applied, it can be seen from Eqs. (24) that the induced stresses are compressive. Also, the induced tangential stresses are quite large in magnitude compared to the induced radial stresses. These induced stress distributions can produce large reduction in the total tangential stresses at the edge of the hole and the stress concentration factor. Figures 2 and 3 confirm the results obtained in Ref. 3 that the stress concentration can be reduced from 3 to 2 (at which point $\theta = 0$ deg becomes critical in compression).

For partial-thickness actuation, the situation is different because of the large radial stresses generated in the plate. Two partial-thickness actuation cases of bonded actuators are shown. For $\beta = 1/6$, the actuator thickness is small compared to the thickness of the plate. In the second case, the thicknesses of the actuators and plate are the same, i.e., $\beta = 1/2$. For both cases, the induced stress distributions are completely different from that obtained with the full-thickness actuation. We can see from Eqs. (23) that near the hole the radial induced stress is larger than the induced tangential stress by a factor of $1/\nu$. When we apply negative actuation strains, the induced radial stresses in the plate increase near the edge of the hole. This increases the stress concentration factor for both criteria, as shown in Figs. 2 and 3, even though the total tangential stress decreases. Positive actuation strains, on the other hand, induce tensile stresses in the plate, and as we can see from Fig. 2, the SCF based on maximum shear-stress criterion increases with the applied actuation strains. However, the SCF based on the Von-Mises stress criterion, as can be seen from Fig. 3, decreases as we increase the applied actuation strain. But the decrease in stress concentration factor with partial-thickness actuation is quite small compared to the full-thickness actuation case. Similar results were obtained with embedded actuators also. Stresses in the actuators are similar to those obtained in the plate for the full-thickness actuation.

Thus, it can be seen that the partial-thickness actuation is ineffective for axisymmetric distribution. This is due to the large radial stresses produced by the actuators. This is in marked contrast to the full-thickness actuation (Ref. 3) where the stress concentration factor could be reduced from 3 to 2 by axisymmetric distributions. Thus, with partial-thickness actuation stress concentration reduction can be achieved only with asymmetric actuation.[5]

Acknowledgments

This research was supported by U.S. Army Research Office Grant DAAL03-92-G-0180 and NASA Grant NAG-1-168.

References

[1]Lin, M. W., and Rogers, C. A., "Analysis of Stress Distribution in a Shape Memory Alloy Composite Beam," AIAA Paper 91-1164-CP; see also *Proceedings of the AIAA/ASME/ASCE/AHS/ASC 32nd Structures, Structural Dynamics, and Materials Conference*, Part 1, AIAA, Washington, DC, 1991, pp. 169–177.

[2]Crawley, E. F., and de Luis, J., "Use of Piezoelectric Actuators as Element of Intelligent Structures," *AIAA Journal*, Vol. 25, No. 10, 1987, pp. 1373–1385.

[3]Sensharma, P. K., Palantera, M. J., and Haftka, R. T., "Stress Reduction in an Isotropic Plate with a Hole by Applied Induced Strains," *Proceedings of the AIAA/ASME/ASCE/AHS/ASC 33rd Structures, Structural Dynamics, and Materials Conference*, Part 2, AIAA, Washington, DC, 1992, pp. 905–913 (AIAA Paper 92-2525).

[4]Timoshenko, S. P., and Goodier, J. N., *Theory of Elasticity*, 3rd ed., McGraw Hill, New York, 1951, Chap. 4.

[5]Sensharma, P. K., and Haftka, R. T., "Limit of Stress Reduction in a Plate with a Hole using Piezoelectric Actuators," *Proceedings of the 1993 ASME Winter Annual Meeting* (New Orleans, LA), Vol. 35, Nov. 1993, pp. 157–164.

Buckling and Vibration Analysis of Skew Plates by the Differential Quadrature Method

X. Wang,* A. G. Striz,† and C. W. Bert‡
University of Oklahoma, Norman, Oklahoma 73019

Introduction

THERE are no known closed-form solutions for the buckling and free vibration behavior of skew plates. Therefore, numerical methods must be utilized to solve the problem. The most widely used ones are various Rayleigh-Ritz methods, the Galerkin method, the finite element method, the finite strip method, the finite difference method, and the Lagrangian multiplier method. Although the Rayleigh-Ritz method uses less computational effort

Received March 3, 1993; revision received Aug. 10, 1993; accepted for publication Aug. 10, 1993.

*Visiting Assistant Professor, School of Aerospace and Mechanical Engineering; currently at the Aircraft Engineering Department, Nanjing University of Aeronautics and Astronautics, Nanjing, People's Republic of China.

†Associate Professor, School of Aerospace and Mechanical Engineering, 865 Asp Avenue. Associate Fellow AIAA.

‡Director and Perkinson Chair Professor, School of Aerospace and Mechanical Engineering, 865 Asp Avenue. Fellow AIAA.

as compared with finite difference and finite element methods, it is often difficult to choose suitable deflection functions that satisfy the general boundary conditions of skew plates.

Recently, the differential quadrature (DQ) method, originated by Bellman and Casti,[1] has been applied to the structural problems of deflection, buckling, and free vibration of beams and circular and rectangular plates.[2,3] The DQ method, using a polynomial to approximate the partial derivative of a function and satisfying boundary conditions on a point-wise basis, solves directly the partial differential governing equation with prescribed boundary conditions for a particular problem. New developments have been made by the present authors in applying the boundary conditions and in the determination of the weighting coefficients, and excellent results were obtained by this approach.[4,5]

This Note presents the analyses of buckling and free vibration of skew plates with simply supported and clamped boundary conditions by the DQ method. Comparisons are made with existing numerical results for frequencies and buckling load, and excellent agreement is achieved.

Differential Quadrature

For simplicity, consider a one-dimensional function $w(x)$ in the $[-1,1]$ domain. In the DQ method, the first derivative at grid point i is approximated as

$$\left.\frac{dw}{dx}\right|_{x=x_i} = w_i' = \sum_{j=1}^{N} A_{ij} w_j, \qquad i = 1, 2, \ldots, N \tag{1}$$

where N = number of grid points, A_{ij} = weighting coefficients of the first derivative, $w_j = w(x_j)$, $x_j = x$ coordinate at grid point j with $x_1 = -1$ and $x_N = 1$.

The A_{ij} are uniquely determined by requiring that Eq. (1) be exact when $w(x)$ takes the following form, i.e.,

$$w(x) = x^{k-1}, \qquad k = 1, 2, \ldots, N \tag{2}$$

Substituting Eq. (2) into Eq. (1) yields

$$(k-1)\, x_i^{k-2} = \sum_{j=1}^{N} A_{ij} x_j, \qquad i, k = 1, 2, \ldots, N \tag{3}$$

Equation (3) represents N sets of N linear equations which can be solved for N^2 weighting coefficients A_{ij}. If Eq. (2) is replaced by

$$w(x) = \left\{1, \sin \pi z, \cos \pi z, \sin 2\pi z, \cos 2\pi z, \ldots, \sin \frac{N-1}{2} \pi z, \cos \frac{N-1}{2} \pi z\right\} \tag{4}$$

where $z = (x+1)/2$ and N is implied to be an odd number, then this version is called harmonic differential quadrature (HDQ).[5]

The DQ method is similar to a mixed collocation method. Since the residual in the collocation method is minimized for ordinary differential equations if the roots of the Chebyshev polynomials are used as collocation points, the grid spacing becomes

$$x_k = \{1, \cos(2i-1)\pi/2N, -1\},$$

$$(i = 2, 3, \ldots, N-1;\ k = N, N-1, \ldots, 2, 1) \tag{5}$$

For the case of plates clamped at both edges,

$$x_k = \{1, 1-\delta, \cos(2i-3)\pi/2(N-2), -1+\delta, -1\},$$

$$(i = 3, 4, \ldots, N-2;\ k = N, N-1, \ldots, 2, 1) \tag{6}$$

where δ is a very small number.[2,3]

Experience shows that by using Eqs. (5) or (6) in the DQ method, reliable results are obtained when the solutions are sensitive to the grid spacing. This also yields much better results for higher-order frequencies.

Application

Consider a thin, isotropic, skew plate of constant thickness h, as in Fig. 1a. The governing differential equation for small-amplitude flexural vibration is

$$w_{,\xi\xi\xi\xi} - (4\cos\theta)\, w_{,\xi\xi\xi\eta} + 2(1 + 2\cos^2\theta)\, w_{,\xi\xi\eta\eta} - (4\cos\theta)\, w_{,\xi\eta\eta\eta} + w_{,\eta\eta\eta\eta} = (\rho h \omega^2/D)\sin^4\theta \tag{7}$$

where θ = skew angle shown in Fig. 1a, ρ = density, ω = circular natural frequency, and D = flexural rigidity. The simply supported boundary conditions are

$$w = 0,\ w_{,\xi\xi} - 2w_{,\xi\eta}\cos\theta = 0 \quad \text{at} \quad \xi = 0, a \tag{8a}$$

$$w = 0,\ w_{,\eta\eta} - 2w_{,\xi\eta}\cos\theta = 0 \quad \text{at} \quad \eta = 0, b \tag{8b}$$

The clamped boundary conditions are

$$w = 0,\ w_{,\xi} = 0 \quad \text{at} \quad \xi = 0, a \tag{9a}$$

$$w = 0,\ w_{,\eta} = 0 \quad \text{at} \quad \eta = 0, b \tag{9b}$$

Table 1a Nondimensional fundamental frequency $\bar{\omega}$ of flexural vibration of rhombic plates vs corner angle θ [SS-SS-SS-SS; $\bar{\omega} = (\omega a^2/\pi^2)\sqrt{\rho h/D}$, $a/b = 1.0$][a]

90 deg		75 deg		60 deg		45 deg	
Leissa (1969)	2.00	Durvasula (1968)	2.11	Durvasula (1968)	2.52	Durvasula(1968)	3.53
Liew and Lam[6]	2.00	Liew and Lam[6]	2.11	Liew and Lam[6]	2.54	Liew and Lam[6]	3.54
DQM ($N = 9$)	2.00	DQM ($N = 9$)	2.11	DQM ($N = 9$)	2.52	DQM ($N = 9$)	3.52
HDQ ($N = 9$)	2.00	HDQ ($N = 9$)	2.11	HDQ ($N = 11$)	2.52	HDQ ($N = 11$)	3.48

[a]All dated references in the table can be found in Ref. 6.

Table 1b Nondimensional fundamental frequency $\bar{\omega}$ of flexural vibration of rhombic plates vs aspect ratio $\bar{b}/\bar{a}$ (SS-SS-SS-SS; $\bar{\omega} = \omega \bar{a}^2\sqrt{\rho h/D}$)

$\bar{b}/\bar{a}$	1.0	1.25	1.50	1.75	2.0	2.25	2.50	2.75	3.0
Gorman[7]	9.870	8.011	6.902	6.170	5.640	5.244	4.940	4.70	4.507
DQM ($N = 9$)	9.870	8.015	6.910	6.182	5.668	5.289	5.001	4.78	4.60
HDQ ($N = 11$)	9.870	8.012	6.902	6.167	5.641	5.243	4.928	4.673	4.463

Table 2 Higher-order frequencies ($\bar{\omega}$) of flexural vibration of SS-SS-SS-SS rhombic plates ($\bar{\omega}^2 = \rho\bar{a}^4\omega^2/D$; $N = 11$)

$\bar{b}/\bar{a}$		2	3	4	5	6	7
1.0	HDQ	24.67	24.67	39.48	49.35	49.35	64.15
	Gorman[7]	24.67	24.67	39.48	49.35	49.35	64.15
1.5	HDQ	15.28	19.23	24.77	34.28	36.98	37.47
	Gorman[7]	15.28	19.22	24.96	34.28	36.98	37.43
2.0	HDQ	11.46	16.81	17.85	25.70	27.76	32.72
	Gorman[7]	11.46	16.78	17.86	25.70	27.76	32.67
2.5	HDQ	9.428	14.17	15.44	19.84	24.16	25.99
	Gorman[7]	9.423	14.17	15.41	19.86	24.08	25.99
3.0	HDQ	8.182	11.92	14.56	16.32	21.08	21.89
	Gorman[7]	8.178	11.91	14.50	16.35	21.07	21.84

Table 3 Buckling coefficients, K ($= N_x b^2/\pi^2 D$), for skew plates with aspect ratio $a/b = 1.0$ (i.e., rhombic plates)[a]

Researchers	Skew angle θ, deg 90	75	60	45	Numerical methods
		Clamped plates (C-C-C-C)			
Guest (1951)	—	—	13.53	20.72	Lagrangian multiplier method
Argyris (1966)	10.15	—	13.76	20.44	FEM (144 elements, 415 unknowns)
Durvasula (1970)	10.08	10.87	13.58	20.44	Galerkin method (18 × 18 matrix)
Prabhu and Durvasula (1972)	10.08	10.87	13.54	20.22	Rayleigh-Ritz
Wang et al.[8]	10.08	10.89	13.75	20.69	pb-2 Rayleigh-Ritz
Present authors	10.08	10.84	13.53	20.61	DQMN ($N = 11$)
Present authors	10.07	10.84	13.54	20.23	DQM ($N = 11$)
		Simply supported plates (SS-SS-SS-SS)			
Fried and Schmitt (1972)	4.00	--	5.91	10.2	FEM
Kennedy and Prabhakara (1979)	4.00	4.33	5.53	8.47	Rayleigh-Ritz
Mizusawa et al. (1980)	4.00	4.34	5.61	8.64	Lagrangian multiplier method
Hegedus (1988)	4.00	4.43	6.16	11.45	Finite strip method
Wang et al.[8]	4.00	4.39	5.98	9.87	pb-2 Rayleigh-Ritz (type 1 corner)
Wang et al.[8]	4.00	4.44	6.19	10.60	pb-2 Rayleigh-Ritz (type 2 corner)
Present authors	4.00	4.40	6.00	9.16	DQMU ($N = 9$)
Present authors	4.00	4.39	5.87	9.79	DQM ($N = 9$)

[a]All dated references in the table can be found in Ref. 8.

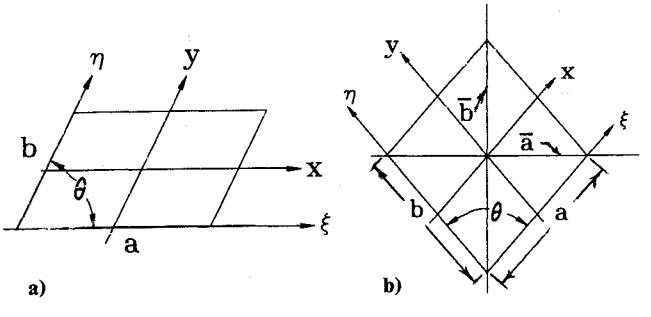

Fig. 1 Skew and rhombic plates.

Let $x = (2\xi - a)/a$ and $y = (2\eta - b)/b$ be nondimensional coordinates; then, application of DQ to Eq. (7) yields

$$\{[\bar{D}^x] - (4\beta\cos\theta)[\bar{C}^x][\bar{A}^y] + 2\beta^2(1 + 2\cos^2\theta)[\bar{B}^x][\bar{B}^y] - (4\beta\cos\theta)[\bar{A}^x][\bar{C}^y] + \beta^4[\bar{D}^y]\}\{w\} = (\bar{\omega}^2/16)\{w\} \quad (10)$$

where $\beta = a/b$, $\bar{\omega}^2 = (\rho h a^4\omega^2/D)\sin^4\theta$, and $\{w\}$ is the displacement vector. Appropriate boundary conditions have been taken into consideration by the method described previously and are incorporated in $\bar{A}$, $\bar{B}$, $\bar{C}$, and $\bar{D}$.

For plates subjected to uniaxial compression (N_x) along the x direction, the right-hand side of Eq. (10) should be replaced by $-(N_x \sin^4\theta/4)(a^2/D)[\bar{B}^x]\{w\}$. In the case of rhombic plates, as shown in Fig. 1b, $\beta \equiv 1$, $\theta = 2\tan^{-1}(\bar{a}/\bar{b})$, and $a = b = (\bar{a}^2 + \bar{b}^2)^{1/2}$.

Results and Comparisons

The fundamental frequencies of simply supported rhombic plates are obtained by both DQM and HDQ, as listed in Table 1a. Equation (5) is used to calculate x_i. The results compare very well with data obtained by other researchers[6,7] (quoted by Liew and Lam[6] for skew plates). It can be seen from Table 1b that the differences between the DQM and HDQ results and Gorman's numerical data become larger with the decrease of skew angle θ (or increase of $(\bar{b}/\bar{a})$; thus, larger N should be used. Results by the HDQ method (for simply supported rhombic plates) are shown in Table 2, which are all close to the data reported by Gorman.[7]

Buckling coefficients by the method are listed in Table 3 for clamped and simply supported skew plates ($a/b = 1$), together with results by other researchers quoted by Wang et al.[8] All dated references in Table 3 can be found in Ref. 8. Both uniform inner grid spacing (DQMN and DQMU)[4] and nonuniform grid spacing (DQM) are used in the calculations. As can be seen, all results are close to each other and insensitive to the method. The results by DQM are close to the Rayleigh-Ritz solution by Prabhu and Durvasula (1972).

For the simply supported case, there is a relatively large variation of results by different researchers when the skew angle θ is less than 75 deg. The DQ results are close to the finite element method results by Argyris (1966) and Fried and Schmitt (1972) and the $pb - 2$ Rayleigh-Ritz (type 1 corner) results by Wang et al.[8] As can be seen, the DQ method yields reliable results for all cases considered.

Conclusion

As demonstrated by the applications, the DQ method is a practical technique for the free vibration and buckling analyses of skew plates. The DQ solutions are in close agreement with those of previous researchers. Since the DQ method offers a very compact procedure and gives quite accurate results, it appears to be more attractive than the classical Ritz method. For a given grid, the weighting coefficients need only be calculated once, which results in further computational efficiency of the method.

References

[1]Bellman, R. E., and Casti, J., "Differential Quadrature and Long-Term Integration," *Journal of Mathematical Analysis and Applications*, Vol. 34, 1971, pp. 235–238.

[2]Bert, C. W., Jang, S. K., and Striz, A. G., "Two New Approximate Methods for Analyzing Free Vibration of Structural Components," *AIAA Journal*, Vol. 26, No. 5, 1988, pp. 612–618.

[3]Jang, S. K., Bert, C. W., and Striz, A. G., "Application of Differential Quadrature to Static Analysis of Structural Components," *International Journal for Numerical Methods in Engineering*, Vol. 28, No. 3, 1989, pp. 561–577.

[4]Wang, X., and Bert, C. W., "A New Approach in Applying Differential Quadrature to Static and Free Vibrational Analyses of Beams and Plates," *Journal of Sound and Vibration*, Vol. 162, No. 3, 1993, pp. 566–572.

[5]Striz, A. G., Wang, X., and Bert, C. W., "Harmonic Differential Quadrature Method and Applications to Free Vibration Analysis of Rectangular Plates," 2nd U.S. National Congress on Computational Mechanics, Washington, DC, Aug. 1993.

[6]Liew, K. M., and Lam, K. Y., "Application of Two-Dimensional Orthogonal Plate Function to Flexural Vibration of Skew Plates," *Journal of Sound and Vibration*, Vol. 139, No. 2, 1990, pp. 241–252.

[7]Gorman, D .J., "Accurate Free Vibration Analysis of Rhombic Plates with Simply Supported and Fully-Clamped Edge Conditions," *Journal of Sound and Vibration*, Vol. 125, No. 2, 1988, pp. 281–290.

[8]Wang, C. M., Liew, K. M., and Alwis, W. A. M., "Buckling of Skew Plates and Corner Condition for Simply Supported Edges," *Journal of Engineering Mechanics*, Vol. 118, No. 4, 1992, pp. 651–662.

Book Reviews

Supercomputing in Fluid Flow

T. K. S. Murthy and C. A. Brebbia (eds.), Computational Mechanics Publications, Boston, and Elsevier Science Publishers (UK) Ltd., New York, 1993, 351 pp., $180.00.

This book contains the written versions of the all-invited papers presented at the International Seminar on Supercomputing in Fluid Flow, held Oct. 3-5, 1989. While there is no lack of gatherings calling themselves international, this one has some right to claim this title since the editors succeeded in bringing together authors from nine countries. These authors contributed 14 papers (or chapters, as they are called in the book) on the development of Euler and Navier-Stokes solvers and/or their application to a variety of flow problems.

The first chapter, by R. A. Shapiro, gives a flavor of what it takes to exploit the computing power of relatively inexpensive, massively parallel processing computers through a rather detailed description of the tailoring of a standard finite-element method for the two-dimensional Euler equations to a CM-2 computer. Shapiro's paper is complemented by a chapter contributed by W. Gentzsch, who formulates some general guidelines for restructuring computational fluid dynamics (CFD) algorithms for vector and parallel computers. A third paper that emphasizes programming issues is by P. Guillen and M. Dormieux, who describe a software package that solves the three-dimensional Euler equations for ideal or real gases on block-structured grids using a wide array of different spatial and temporal discretization concepts; some of their first results are included.

Readers more interested in computational methods rather than their programming might enjoy E. Dick's review of his polynomial flux-difference splitting concept, which applies to both the compressible and the incompressible Euler equations. Another article, by J. Häuser, A. Vinckier, and S. Zemsch, describes in great detail the governing equations for hypersonic flow with non-equilibrium effects and a related computational method. As a note of caution, let it be mentioned that while Dick shows at least some results for two-dimensional flows of low to modest complexity, Häuser, Vinckier, and Zemsch have only a grid to show for computing inviscid flow over a Hermes configuration.

Three chapters deal with applications of CFD in the automotive industry. R. Himeno, K. Fujitani, and M. Takagi show results for unsteady flow over quite complete automobile geometries. T. Kobayashi, Y. Morinishi, and N. Tanaguchi report some large-eddy-simulations for flows about more generic automobile shapes. A. Taklanti presents results for unsteady flows in manifolds and in the combustion chambers of piston engines.

The simulation of three-dimensional viscous flows with and without separation is the topic of four of the entries. A. Rizzi's paper focuses on the simulation of transonic flows over large-aspect ratio wings using a Navier-Stokes solver based on his well-known finite-volume method with Runge-Kutta time-stepping for the Euler equations. Using a related computational method, D. Schwamborn, A. Hilgenstock, H. Zimmermann, and W. Kordulla build on Rizzi's results as they include simulations of massively separated flows over slender configurations. The third paper in this category, by G. B. Deng, Y. Lecointe, J. Piquet, P. Queutey, and M. Visonneau, combines theory and numerical experiments in an unusual way in the analyses of incompressible viscous flow over a tanker hull and over a prolate spheroid. Finally, H. J. Haussling, J. J. Gorski, and R. M. Coleman report on applications of a multi-block finite-volume method for the incompressible Navier-Stokes equations that allows choosing between central differencing and upwinding of the inviscid fluxes as well as between two turbulence models. Their results show a quite impressive agreement between com-